Model Study of Coherent-Control of the Femtosecond Primary Event of Vision†

Samuel C. Flores and Victor S. Batista*

Department of Chemistry, Yale University, PO Box 208107, New Haven, Connecticut 06520-8107

Received: October 9, 2003; In Final Form: January 19, 2004

A bichirped coherent-control scenario is introduced and implemented in a model study of coherent-control of the cis/trans photoisomerization of the retinal chromophore in rhodopsin. The approach involves selective photoexcitation of multiple vibrationally coherent wave packets by using two chirped femtosecond pulses. Control over product yields at finite time after photoexcitation of the system is achieved by externally changing the relative *phases* of the photoexcitation pulses and consequently affecting the interference phenomena between individual wave packet components. Furthermore, a measure of decoherence associated with the underlying quantum reaction dynamics is computed. Extensive coherent-control over transient populations is predicted, despite the ultrafast decoherence phenomena induced by the vibronic activity, providing results of broad theoretical and experimental interest.

I. Introduction

Understanding the role of quantum coherences in intramolecular relaxation processes of biological molecules is a subject of great interest.[1,2] Reactions in biomolecules (e.g., proteins) usually involve intramolecular processes with rearrangements of nuclear and electronic degrees of freedom at a "reaction site", whereas the remainder of the molecular structure provides a regulatory environment (i.e., a "bath") for the underlying reaction dynamics. Quantum mechanical coherences can, therefore, play a crucial role in determining the overall rate and efficiency of the reaction whenever the reaction time is comparable to, or shorter than, the time scale for decoherence induced by the interactions with the bath. In this paper, we investigate the effect of laser induced coherences in the cis/trans photoisomerization reaction of the retinal chromophore in rhodopsin, as modeled by an empirical Hamiltonian. We introduce a bichirped coherent-control scenario, and we computationally demonstrate the possibility of coherently controlling the underlying excited-state reaction dynamics.

Chirped, or shaped, light pulses can efficiently transfer population between different electronic states in polyatomic systems.[3−8] Such population transfer induces selective excitation of coherent wave packet motion with a strong dependence on the chirp sign. Negatively chirped pulses induce vibrational coherences through intrapulse pump−dump processes,[9] whereas positively chirped pulses discriminate against the formation of coherences, increasing the excited-electronic state population.[3−8] The bichirped coherent-control scenario introduced in this paper exploits these capabilities of chirped femtosecond pulses. However, contrary to achieving quantum control of transient populations by changing the pulse chirps, coherent-control is achieved by changing the relative *phases* of two linearly chirped femtosecond pulses.

Coherent-control exploits the coherence properties of lasers to encode and manipulate quantum mechanical interferences between multiple photoexcitation pathways leading to the same final state.[10−13] The control parameters for manipulating interferences are the relative *phases* of multiple photoexcitation pulses. Several coherent-control scenarios have been demonstrated both computationally and experimentally for simple reactions in small molecules.[10,11,13] However, coherently controlling intramolecular dynamics in large molecules has often been deemed unrealistic due to the deleterious effects of rapid decoherence.[14] In recent work, we have computationally demonstrated coherent-control of ultrafast excited-state reaction dynamics in a large polyatomic system.[15,16] Coherent-control was found to be feasible, even in the presence of ultrafast intrinsic decoherence, since in that system the excited-state reaction time was comparable to the period of vibrational modes responsible for inducing decoherence.[34]

The time scales for decoherence and reaction dynamics observed in our previous studies are expected to be common to many other excited-state reactions, since the excited-electronic states responsible for reaction dynamics in polyatomic systems are usually extremely short-lived and determine reaction times that are comparable to the periods of the dominant vibrations. In this paper, we investigate the decoherence time scale for the excited-state photoisomerization in rhodopsin as modeled by an empirical Hamiltonian and we show that coherent-control is in fact feasible since the 200-fs reaction time is comparable to the decoherence time.

The cis/trans photoisomerization reaction in rhodopsin is the first step in vision and represents an extremely efficient and ultrafast phototransduction mechanism that has already raised significant interest in the field of bioelectronics[17] (i.e., the subfield of molecular electronics that investigates the utility of native as well as modified biological molecules in electronic or photonic devices). In addition to the obvious advance associated with demonstrating coherent-control of such reaction, the bichirped coherent-control scenario also provides a technique for significantly improving our understanding of the role of quantum coherences in intramolecular relaxation processes of polyatomic systems.

The paper is organized as follows. Section II describes the system, the computational approach and the implementation of the bichirped coherent-control scenario. Section III presents results for both coherent-control as a function of the pulse

† Part of the special issue "Hans C. Andersen Festschrift".

* To whom correspondence should be addressed.

10.1021/jp0370526 CCC: $27.50
Published on Web 03/02/2004

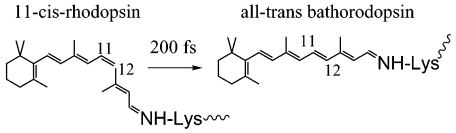

Figure 1. Photoisomerization of retinal in rhodopsin.

relative phases and for a time- dependent decoherence measure. Section IV summarizes and concludes.

II. Methods

The cis/trans photoisomerization of the retinal chromophore in rhodopsin, shown in Figure 1, is complete with high efficiency (~67%) within 200 fs after photoexcitation of the system.[1,2] The reaction involves torsional motion of the dihedral angle about the $C_{11}-C_{12}$ bond (see Figure 1) through a diabatic pathway that connects the excited-electronic state of the 11-cis-rhodopsin with the ground-electronic state of the all-trans photoproduct. The two electronic states are vibronically coupled, primarily by the delocalized stretching motion of the polyene chain in the retinal chromophore. A microscopic description of the underlying intramolecular reaction dynamics thus requires modeling both nuclear and electronic relaxation dynamics on vibronically coupled potential energy surfaces.

Previous studies[18,19] have shown that most of the available spectroscopic information on rhodopsin can be properly described by simulating the underlying quantum dynamics according to an empirical two-state 25-mode model Hamiltonian $\hat{H} = \hat{H}_M + \hat{H}_B$. Here, $\hat{H}_M$ is a two-state two-mode model Hamiltonian that accounts for the collective torsional coordinate and its coupling to the delocalized stretching mode of the polyene chain, whereas $\hat{H}_B$ is a harmonic ansatz (i.e., the "bath") with frequencies and excited-state gradients parametrized to reproduce the experimental resonance Raman excitations of rhodopsin.[20] The $\hat{H}_M$ term is parametrized to reproduce the rhodopsin electronic excitation energies, as well as the energy stored and the spectroscopic energy shift due to the isomerization of the retinyl chromophore in rhodopsin. In addition to reproducing all of these experimental data by construction, the model Hamiltonian properly describes the isomerization reaction speed, efficiency (i.e., the quantum product yield) and the femtosecond spectroscopic signals during the first picosecond of dynamics as correlated to time-dependent populations of the model potential energy surfaces. In this paper, such a model is implemented to explore the feasibility of coherently controlling the reaction efficiency. Specifically, we analyze the sensitivity of the reaction efficiency to changes in the coherent properties of femtosecond pump pulses. Note, that we have cautiously limited our coherent-control study to the analysis of the very same quantities for which the model Hamiltonian has been demonstrated to be useful.

The dynamics of the system is generated by the total Hamiltonian $\bar{H}(t) = \hat{H} + \hat{V}(t)$, where $\hat{H} = \hat{H}_M + \hat{H}_B$ and $\hat{V}(t)$ is the perturbation due to the time-dependent laser-field $\epsilon(t)$

$$\hat{V}(t) = -|1\rangle\langle 0|\, \epsilon(t)\cdot\hat{\mu} - |0\rangle\langle 1|\, \epsilon(t)\cdot\hat{\mu} \tag{1}$$

where $\hat{\mu}$ is the dipole operator and $|0\rangle$ and $|1\rangle$ are the ground- and excited-electronic states of rhodopsin, respectively.

The TDSCF approach[18,21−23] is implemented by employing a single-configuration Hartree ansatz

$$\Psi(\xi,\phi,R,\mathbf{x};t) = e^{i\eta(t)}\chi(\xi,\phi,R;t)\phi(\mathbf{x};t) \tag{2}$$

where ϕ is the isomerization coordinate, R is the delocalized stretching mode of the polyene chain and $\mathbf{x}$ are the remaining 23 resonance Raman active modes included in the model, $\eta(t)$ is an overall phase factor, and $\xi = 0, 1$ labels the ground- and excited-electronic states of rhodopsin, respectively. Substituting the ansatz introduced by eq 2 into the time-dependent Schrödinger equation, we obtain the well-known self-consistent field equations[18,21−23]

$$i\hbar\dot{\phi}(\mathbf{x},t) = \langle\chi|\,\bar{H}\,|\chi\rangle\phi(\mathbf{x},t) \tag{3}$$

and

$$i\hbar\dot{\chi}(\xi,\phi,R;t) = \langle\phi|\,\bar{H}\,|\phi\rangle\chi(\xi,\phi,R;t) \tag{4}$$

Since the Hamiltonian $\hat{H}_B$ is harmonic, $\phi(\mathbf{x},t)$ can be described in terms of Gaussian wave packets

$$\phi(\mathbf{x};t) = \prod_j\left(\frac{1}{\pi}\right)^{-1/4}\exp\left[-\frac{1}{2}(x_j - x_j(t))^2 + \frac{i}{\hbar}(p_j(t)(x_j - x_j(t)) + S(t))\right] \tag{5}$$

where $\{x_j(t),\ p_j(t)\}$ are classical vibrational coordinates and momenta that evolve according to the effective potential energy surface $V_{\text{eff}}(\mathbf{x}) = \langle\chi|\,\bar{H}\,|\chi\rangle$. These trajectories are computed along with the classical action $S(t)$ by numerically integrating Hamilton's equations according to the Velocity−Verlet algorithm.[24] Finally, eq 4 is solved self-consistently with eq 3 by implementing an exact quantum dynamics propagation scheme based on the split-operator Fourier transform method.[25,26] For a discussion of the validity of the TDSCF method as implemented here, see refs 18 and 21−23.

The system is initially prepared in the ground-electronic state and is photoexcited with two linearly chirped femtosecond pulses with a total electric field $\epsilon(t)$

$$\epsilon(t) = F_1(t)e^{-i(\omega_1 t+\theta_1)} + F_2(t)e^{-i(\omega_2 t+\theta_2)} + \text{c.c.} \tag{6}$$

where θ_j are the phases of the two pulses and c.c. denotes the complex conjugate of the preceding terms. The functions F_j, introduced by eq 6, describe Gaussian pulses

$$F_j(t) = F_{\max}\exp\left(-\frac{t^2}{2}\left(\frac{1}{t_p^{\,2}} + i\frac{1}{\tau_j^{\,2}}\right)\right) \tag{7}$$

where the parameters t_p and τ_j, introduced by eq 7, describe the temporal width and the linear chirp rates, respectively.[35] The two pulse components include a negatively chirped pulse, responsible for creating vibrational coherences and a positively chirped component that discriminates against the formation of coherences. Hence, in this bichirped femtosecond version of coherent-control, selectively excited-vibrational coherences interfere with one another and such quantum mechanical interference phenomena affect the time dependent reactant and product populations.

We focus our study on the analysis of both the probabilities $P_{\text{cis}}^{(S_1)}(t)$ and $P_{\text{trans}}^{(S_0)}(t)$ of the system to be in the cis configuration of the S_1 excited-electronic state and the trans configuration in the ground-electronic state, respectively. The populations of these two states can be directly correlated to transient signals in femtosecond pump−probe experiments at probe wavelengths in the 500 and 530−580 nm ranges, respectively.[2] It is, therefore, expected that the results predicted by our calculations could be experimentally verified by femtosecond laser spectroscopy.

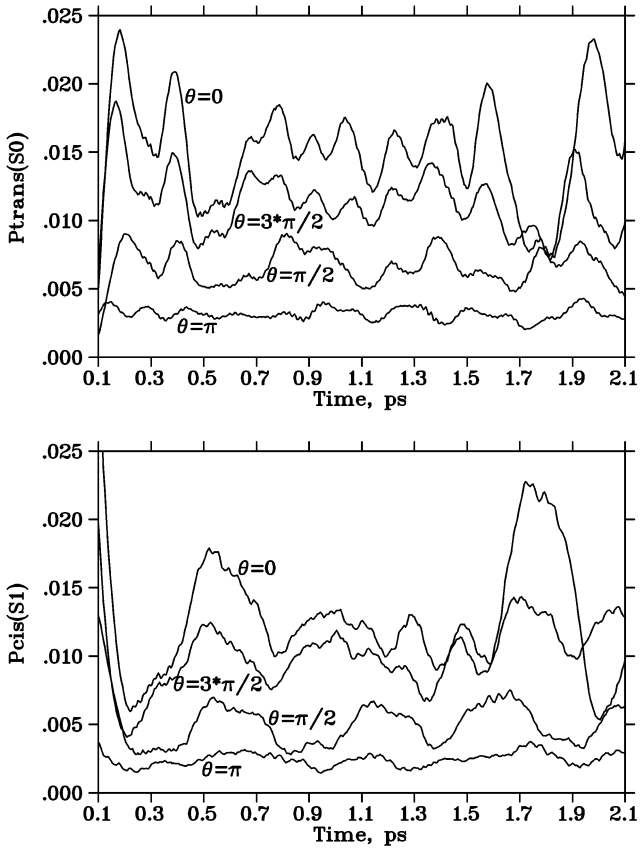

Figure 2. Time-dependent probability of the system to be in the trans configuration of the S_0 electronic state, $P_{\text{trans}}^{(S_0)}(t)$ (upper panel), and the cis configuration of the S_1 electronic state, $P_{\text{cis}}^{(S_1)}(t)$ (lower panel), for relative pump pulse phases $\theta = 0$, $3\pi/2$, $\pi/2$, and π.

We compute $P_{\text{cis}}^{(S_1)}(t)$, as a function of the relative pulse phase parameter $\theta = \theta_1 - \theta_2$, as follows:

$$P_{\text{cis}}^{(S_1)}(t) = \langle \Psi_t^{(S_1)} | \, h_{\text{cis}}(\phi) \, | \Psi_t^{(S_1)} \rangle \tag{8}$$

where $|\Psi_t^{(S_1)}\rangle \equiv |S_1\rangle\langle S_1|\Psi_t\rangle$ is the S_1 electronic component of the time-evolved wave function $|\Psi_t\rangle$ and $h_{\text{cis}}(\phi)$ is a function of the dihedral angle ϕ about the $C_{11}-C_{12}$ bond, defined as $h_{\text{cis}}(\phi) = 1$ when $|\phi| \leq \pi/2$, and 0 otherwise. The time-dependent populations $P_{\text{cis}}^{(S_0)}$, $P_{\text{trans}}^{(S_1)}$, and $P_{\text{trans}}^{(S_0)}$ are computed analogously.

We consider the system initially prepared in the ground-harmonic state for all nuclear degrees of freedom. The frequencies introduced by eq 6 are $\omega_1 = \omega_2 = 2\pi c/\lambda$ with $\lambda = 500$ nm. The parameters that define the pump pulse temporal profiles, introduced by eq 7, are $t_p = 42$ fs, $\tau_1^2 = 576$ fs^2, and $\tau_2^2 = -1156$ fs^2. We focus on the weak-field limit by selecting the maximum field strength $F_{\text{max}} = 0.25$ MeV/cm for both pump pulses. The net effect of the field is rather weak due to the brevity of the pulse: less than 4% of the population is transferred from the ground- to the excited-electronic state. Note that by fixing the parameters that define $F_1(t)$ and $F_2(t)$ one can simultaneously explore all possible outcomes that result from different values of the coherent-control parameter $\theta = \theta_1 - \theta_2$. Here, we do not explore the influence of the field strength,[27] relative intensities, chirp rates, or pulse widths. However, the parameters that define such quantities in the real bichirped coherent-control experiment could be optimized, e.g., according to a closed-loop optimal-control scheme.[12,28−31]

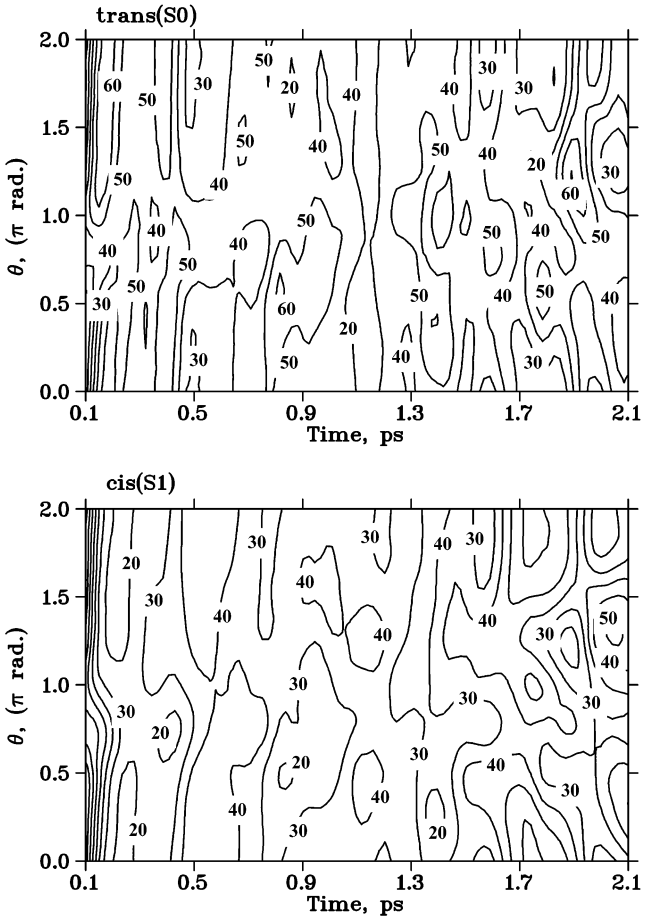

Figure 3. Contour plots of trans-S_0 (upper panel) and cis-S_1 (lower panel) time-dependent percentage populations for bichirped coherent control of rhodopsin as a function of the relative phase $\theta = \theta_1 - \theta_2$ of the photoexcitation pulses.

III. Results

Figure 2 compares $P_{\text{trans}}^{(S_0)}$ (upper panel) and $P_{\text{cis}}^{(S_1)}$ (lower panel) for various different values of the relative pulse phase parameter θ.

These results show evidence of significant changes in the dynamics of cis/trans photoisomerization in rhodopsin produced solely by changes in the relative pulse laser parameter θ. Note that both the excited- and ground-state recurrences are strongly modulated by θ in terms of their timing, spreading, and relative intensities. The origin of such recurrences is the refocusing of excited- and ground-state populations back to the cis and trans conformations, respectively, after the S_1 population bifurcates at a conical intersection of the relevant potential energy surfaces (for an earlier discussion of photoisomerization and internal conversion at conical intersections, see ref 32). The bifurcation event gives rise to both the first peak of $P_{\text{trans}}^{(S_0)}$ and the first minimum of $P_{\text{cis}}^{(S_1)}$, shown in Figure 2 at about 200 fs after photoexcitation of the system.

Figure 3 shows contour plots of trans-S_0 (upper panel) and cis-S_1 (lower panel) time-dependent percentage populations, defined as $100*P_{\text{trans}}^{(S_0)}(t)/P_{\text{tot}}$ and $100*P_{\text{cis}}^{(S_1)}(t)/P_{\text{tot}}$, respectively. Here, P_{tot} is the total population transferred from the ground- to the excited-electronic state by the photoexcitation pulses.

Figure 3 shows that coherent control is feasible simply by changing the relative phases of the photoexcitation pulses. Note that the reaction efficiency (i.e., the trans-S_0 percentage population) can be modulated from more than 60% to less than 30% by changing the coherent control parameter θ.

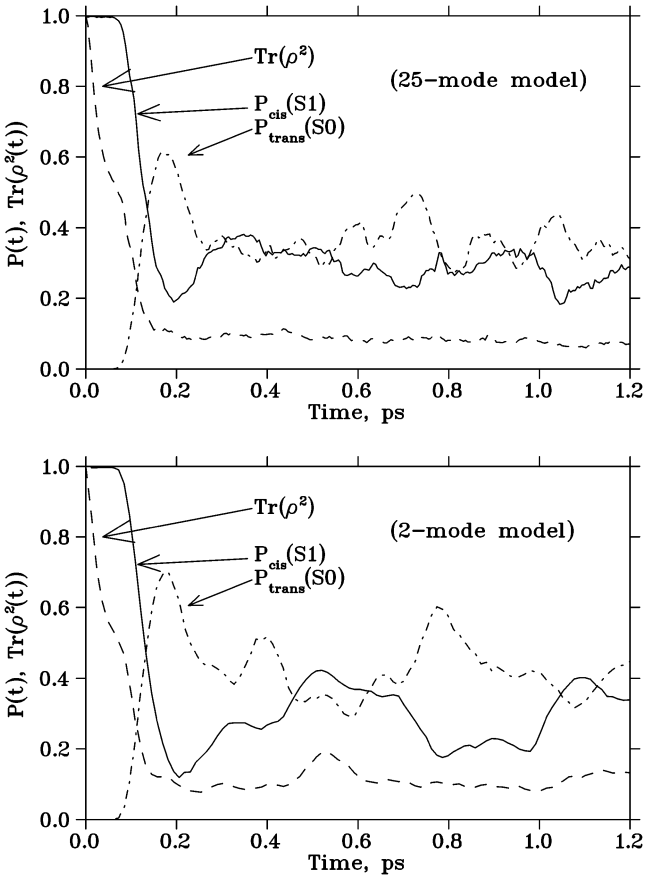

Figure 4. Comparison of the evolution of the $\mathrm{Tr}[\rho^2]$ (dashes) with the evolution of the time-dependent reactant cis-S_1 (solid lines) and trans-S_0 (broken dashes) populations during the first 1.2 ps of dynamics after photoexcitation of the system.

The extent to which these results are significant is associated with the advent of intrinsic decoherence, induced by the coupling between the reaction coordinate (i.e., the torsion of the dihedral angle about the $C_{11}-C_{12}$ bond) and the stretching mode of the polyene chain. We estimate the decoherence rate, according to our previous work,[15] by computing the time-dependent $\mathrm{Tr}[\rho^2(t)]$ where $\rho(t)$ is the reduced density matrix associated with the reaction coordinate. The calculation is performed for a harmonic state initially promoted to the S_1 excited-electronic state. Since the decoherence rate is expected to increase with the configuration space size, such an initial condition serves as an approximate lower bound to the decoherence rate. According to such preparation, the system is initially in a pure state, i.e., $\mathrm{Tr}[\rho^2(0)] = 1$. However, as the isomerization reaction proceeds, the torsional motion of the dihedral angle becomes coupled to the motion of the remaining degrees of freedom in the system (i.e., the stretching mode of the polyene chain and the remaining 23 vibrationally active modes) and $\mathrm{Tr}[\rho^2(t)]$ decays at the decoherence rate. Figure 4 (upper panel) shows the time-evolution of $\mathrm{Tr}[\rho^2(t)]$ and the comparison with the evolution of both $P_{\mathrm{cis}}^{(S_1)}$ and $P_{\mathrm{trans}}^{(S_0)}$ during the first 1.2 ps of dynamics.

The lower panel of Figure 4 shows the analogous results for a two-state two-mode model Hamiltonian constructed by turning off the coupling to the harmonic ansatz. The comparison of $\mathrm{Tr}[\rho^2(t)]$ for the 25-mode model (upper panel) and the 2-mode model (lower panel) suggests that the main contribution to decoherence is due to the coupling of the reaction coordinate to the stretching mode of the polyene chain. Note that during the early time relaxation ($t < 70$ fs) most of the population remains on the reactant side of the initially populated electronic state (i.e., $P_{\mathrm{cis}}^{(S_1)} \approx 1$). However, $\mathrm{Tr}[\rho^2]$ rapidly decays due to the intrinsic decoherence induced by the vibronic activity and reaches a plateau as soon as the reaction is complete at 200 fs.

IV. Summary and Conclusions

We have introduced a bichirped coherent-control scenario, and we have computationally demonstrated the feasibility of coherently controlling the femtosecond primary event of vision as modeled by an empirical Hamiltonian that properly describes the underlying reaction speed and efficiency. Considering the longstanding research interest in rhodopsin photoisomerization, we anticipate considerable experimental interest in examining this coherent-control scenario.

We have shown that the coupling between the reaction coordinate and the stretching mode of the polyene chain in the retinal chromophore induces decoherence within a time scale comparable to the reaction time. To our knowledge, these results and those reported earlier[15] constitute the first explicit calculations of the time-dependent $\mathrm{Tr}[\rho^2]$ associated with excited-state reaction dynamics in polyatomic molecules. Such quantity is the standard and most conventional measure of decoherence.

We have shown that the predicted range of control is extensive despite the ultrafast intrinsic decoherence induced by the vibronic activity, providing results of broad theoretical and experimental interest.

Acknowledgment. V.S.B. acknowledges a generous allocation of supercomputer time from the National Energy Research Scientific Computing Center and financial support from a Research Innovation Award from Research Corporation, a Petroleum Research Fund Award (type G) from the American Chemical Society, a junior faculty award from the F. Warren Hellman Family, and start-up package funds from the Provost's office at Yale University. The authors thank Mr. Yinghua Wu, Mr. Sabas Abuabara and Dr. Julian Tirado-Rives for their assistance and advice.

References and Notes

(1) Schoenlein, R.; Peteanu, L.; Mathies, R.; Shank, C. *Science* **1991**, *254*, 412.
(2) Wang, Q.; Schoenlein, R.; Peteanu, L.; Mathies, R.; Shank, C. *Science* **1994**, *266*, 422.
(3) Bardeen, C.; Wang, Q.; Shank, C. *Phys. Rev. Lett.* **1995**, *75*, 3410.
(4) Bardeen, C.; Yakovlev, V.; Squier, J.; Wilson, K. *J. Am. Chem. Soc.* **1998**, *120*, 13023.
(5) Cerullo, G.; Bardeen, C.; Wang, Q.; Shank, C. *Chem. Phys. Lett.* **1996**, *262*, 362.
(6) Bardeen, C.; Cao, J.; Brown, F.; Wilson, K. *Chem. Phys. Lett.* **1999**, *302*, 405.
(7) Cao, J.; Bardeen, C.; Wilson, K. *Phys. Rev. Lett.* **1998**, *80*, 1406.
(8) Fainberg, B.; Gorbunov, V. *J. Chem. Phys.* **2002**, *117*, 15.
(9) Tannor, D.; Kosloff, R.; Rice, S. *J. Chem. Phys.* **1986**, *85*, 5805.
(10) Shapiro, M.; Brumer, P. In *Advances in Atomic, Molecular and Optical Physics*; Bederson, B., Walther, H., Eds.; Academic Press: San Diego, CA, 2000; pp 287−343.
(11) Shapiro, M.; Brumer, P. *Principles of the Quantum Control of Molecular Processes*; Wiley: New York, 2003.
(12) Rice, S.; Zhao, M. *Optical Control of Molecular Dynamics*; Wiley: New York, 2000.
(13) Gordon, R.; Zhu, L.; Seidman, T. *J. Chem. Phys.* **2001**, *105*, 4387.
(14) Hache, A.; Sipe, J.; van Driel, H. *IEEE J. Quantum Electron.* **1998**, *34*, 1144.
(15) Batista, V.; Brumer, P. *Phys. Rev. Lett.* **2002**, *89*, 143201.
(16) Batista, V.; Brumer, P. *Phys. Rev. Lett.* **2002**, *89*, 249903.
(17) Birge, R.; Gillespie, N.; Izaguirre, E. W.; Kusnetzow, A.; Lawrence, A.; Singh, D.; Song, Q.; Schmidt, E.; Stuart, J.; Seetharaman, S.; Wise, K. *J. Phys. Chem. B* **1999**, *103*, 10746.
(18) Hahn, S.; Stock, G. *Chem. Phys.* **2000**, *259*, 297.
(19) Hahn, S.; Stock, G. *J. Phys. Chem. B* **2000**, *104*, 1146.
(20) Lin, S.; Groesbeek, M.; van-der Hoef, I.; Verdegem, P.; Lugtenburg, J.; Mathies, R. *J. Phys. Chem. B* **1998**, *102*, 2787.

(21) Gerber, R.; Buch, V.; Ratner, M. *J. Chem. Phys.* **1982**, *77*, 3022.
(22) Dirac, P. *Proc. Camb. Philos. Soc.* **1930**, *26*, 376.
(23) Kotler, Z.; Neria, E. *Comput. Phys. Comm.* **1991**, *63*, 234.
(24) Swope, W.; Andersen, H.; Berens, P.; Wilson, K. *J. Chem. Phys.* **1982**, *76*, 637.
(25) Feit, M.; Fleck, J. *J. Chem. Phys.* **1983**, *78*, 301.
(26) Wu, Y.; Batista, V. *J. Chem. Phys.* **2003**, *118*, 6720.
(27) Bartana, U.; Banin, A.; Ruhman, S.; Kosloff, R. *Chem. Phys. Lett.* **1994**, *229*, 211.
(28) Judson, R.; Rabitz, H. *Phys. Rev. Lett.* **1992**, *68*, 1500.
(29) Ohtsuki, Y.; Ohara, K.; Abe, M.; Nakagami, K.; Fujimura, Y. *Chem. Phys. Lett.* **2003**, *369*, 525.
(30) Grossmann, F.; Feng, L.; Schmidt, G.; Kunert, T.; Schmidt, R. *Europhys. Lett.* **2002**, *60*, 201.
(31) Geppert, D.; Hofmann, A.; de Vivie-Riedle, R. *J. Chem. Phys.* **2003**, *119*, 5901.
(32) Seidner, L.; Domcke, W. *Chem. Phys.* **1994**, *186*, 27.
(33) Cao, J.; Wilson, K. *J. Chem. Phys.* **1997**, *107*, 1441.

(34) In the absence of an external bath, decoherence is solely due to the interaction between the reaction coordinate and the remaining degrees of freedom in the molecular structure. Under those circumstances, we refer to *intrinsic decoherence* to make a distinction from decoherence induced by an external bath.

(35) The reference to a "linear chirp rate" refers to the linear correlation between frequency and time. Note that such a correlation cannot be deduced from the correlation between intensity and time, introduced by eq 7. Instead, the frequency-time correlation can be deduced by representing the electric field $\epsilon(t)$ in the Wigner transformation form.[33]